ACS OMEGA

Open Access

http://pubs.acs.org/journal/acsodf

Article

Soft Deposition of Organic Molecules Based on Cluster-Induced Desorption for the Investigation of On-Surface and Surface-Mediated Reactions

Karolin Pluschke, Aaron Herrmann, and Michael Dürr*

Cite This: *ACS Omega* 2023, 8, 40639−40646

Read Online

ACCESS | Metrics & More | Article Recommendations | Supporting Information

ABSTRACT: Desorption/ionization induced by neutral clusters (DINeC) was employed for the soft transfer of organic and biomolecules, such as porphyrins and peptides, from a bulk sample onto any substrate of choice. Qualitative analysis of the deposition technique was performed by means of mass spectrometry, demonstrating that the deposited molecules remained intact due to the soft nature of the transfer process. Deposition rates were studied quantitatively using a quartz crystal microbalance; layers of intact biomolecules ranging from the submonolayer regime up to a few monolayers in thickness were realized. Mixed layers of molecules were deposited when two different sources of molecules were employed. The samples which were prepared based on this soft deposition method were used for the investigation of reactions of the deposited molecules with either coadsorbates on the surface or the surface itself. Examples include adduct formation of peptides with alkali metals on SiO_2, the oxidation of peptides exposed to oxygen, as well as the metallization of porphyrins in interaction with the substrate.

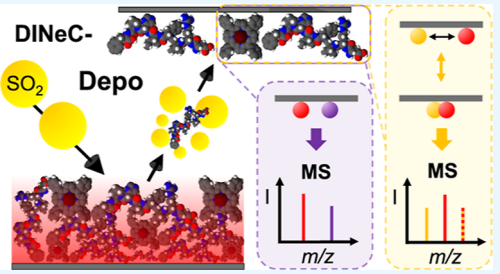

INTRODUCTION

The preparation of thin organic films by means of physical vapor deposition (PVD) is a well-established technique.[1,2] It is applied, e.g., for the preparation of thin films of metal−organic complexes, polymers, or other organic molecules, which are used, among others, in organic solar cells, organic thin film transistors, and organic light-emitting diodes.[3−5] However, PVD is only applicable to molecules that do not decompose at the elevated temperatures used to sublimate the molecules.[6,7] For the deposition of larger, more complex molecules such as biomolecules, a variety of dedicated techniques have been established; most of these techniques originate from (soft) ionization methods used in mass spectrometry (MS). For example, soft landing of molecular ions such as electrospray ion beam deposition (ES-IBD), can be used to deposit intact molecules such as peptides, proteins, and other molecules with layer thicknesses in the submonolayer to the nanometer range.[8−10] Matrix-assisted pulsed laser evaporation (MAPLE), which was derived from matrix-assisted laser desorption/ionization MS, was also applied for the deposition of larger molecules in the 10 to 1000 kDa range.[11] Noble gas cluster ion beams (GCIBs), which are typically employed for soft secondary ion MS, were also used to sputter/deposit intact biomolecules.[12,13] Whereas ES-IBD is limited to the deposition of molecular ions, MAPLE involves the codeposition of the matrix molecules if not only charged molecules are selected. In the case of the deposition induced by GCIB, a finite fraction of fragmented molecules is still expected to be deposited.[14]

In this paper, we show that desorption induced by neutral SO_2 clusters (DINeC), which is an extremely soft desorption method applied in MS,[15−17] can be employed as a deposition technique as well (short: DINeC-Depo). In this application of DINeC, the molecules are softly desorbed from a bulk sample by the SO_2 clusters and deposited directly onto a substrate that is placed opposite to the target (Figure 1a). The soft desorption of the molecules relies on a dissolution-based mechanism:[15,18,19] the impacting clusters do not only provide the energy for desorption but also serve as a transient matrix in which the desorbing molecules are dissolved.[18−20] As a result, the effective desorption barrier is reduced which enables soft desorption with low-energy clusters.[15−17] As most of the SO_2 molecules are evaporating from the desorbed molecules after cluster-surface impact and desorption,[15,20] the bare molecules can be then deposited on a target of choice; as only a minority of the desorbed molecules are ionized,[21] mainly neutral molecules are deposited. Based on the results for DINeC-MS, the DINeC-Depo method can be applied to a broad variety of molecules, e.g., lipids, peptides, proteins, dyes, polymers, and ionic liquids.[20,22−25] The coverage of the deposited layers ranges from isolated molecules in the

Received: July 28, 2023
Accepted: October 2, 2023
Published: October 19, 2023

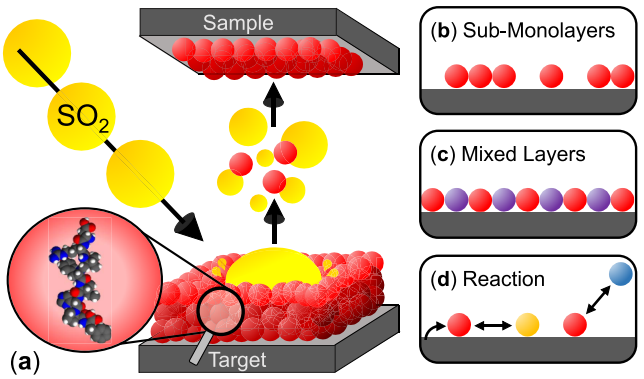

Figure 1. Schematic depiction of the DINeC-Depo experiment: (a) SO_2 clusters hit the surface and desorb the molecules that were drop-cast on the target substrate. The desorbed molecules can be deposited on any surface of choice. (b) Samples in the submonolayer to multilayer regime were prepared. (c) Mixed layers were deposited by using different target molecules. (d) Interactions of the deposited molecules with the surface or other adsorbates were investigated.

submonolayer regime (Figure 1b) to films of the thickness of several monolayers. The sample composition was controlled by changing the target material during the deposition process (Figure 1c). Samples prepared by DINeC-Depo were used to study the interaction of the deposited molecules with the surface of the substrate, with other adsorbates, or with gas phase molecules to which they were exposed (Figure 1d). In general, higher reactivity of the deposited species is observed when compared to molecules in solution or thin films.

EXPERIMENTAL SECTION

The deposition process was performed in a vacuum chamber (base pressure $p \approx 10^{-6}$ mbar), which was set up for this type of experiment (Figure S1 in the Supporting Information). The cluster beam, which was used for the desorption of the target molecules, was generated via supersonic expansion of a gas mixture containing 3% SO_2 in helium (pressure p = 15 bar) using a pulsed nozzle (repetition rate f = 2 Hz, effective opening time t = 300 ms). The clusters, consisting of 10^3 to 10^4 SO_2 molecules, hit the target surface at an angle of 45° with respect to the surface normal; the clusters' velocity $v \approx 10^3$ m/s converts into an energy density of ≈0.8 eV per molecule.[26] The clusters desorb the molecules from the target, which is positioned 90 mm from the nozzle. The substrate, on which the molecules were deposited, was mounted directly opposite to the target at a distance of d_{ST} = 8 to 30 mm. The target consisted of a piece of silicon wafer (2 × 2 cm^2) covered with its natural oxide onto which an aqueous solution ($c = 10^{-3}$ mol/L, V = 100 μL) was drop-cast. Prior to use, all substrates were cleaned in ethanol and acetone in an ultrasonic bath for 15 min each. To remove metal contamination from the silicon oxide surface, some of the substrates were additionally cleaned with the so-called "RCA cleaning procedure type 2" reported by the *Radio Corporation of America*.[27] Peptides (purity >97%) were purchased at Sigma-Aldrich Chemie GmbH, Taufkirchen, Germany, and porphyrins (purity >98%) were purchased at PorphyChem SAS, Longvic, France.

During deposition, the substrate was covered with a deposition mask (perforated metal plate, r_{hole} = 3 mm); the target and sample holder were on ground potential. The deposition rate was determined quantitatively using a quartz crystal microbalance (QCM SR560, QCM200-5 MHz Crystal Oscillator, Stanford Research Systems). Sample transfer from the deposition chamber to the vacuum chamber of the mass spectrometer was carried out through ambient conditions unless stated otherwise.

After deposition, the samples were analyzed by means of DINeC-MS. For the MS measurements, the masks were removed from the samples; the deposited molecules were desorbed by SO_2 clusters in the same way as described for the deposition procedure. In the former case, the desorbed ions were transferred into a commercial ion trap mass spectrometer (amaZon speed from Bruker Daltonik GmbH, Bremen Germany), which was equipped with a custom-built DINeC ion source; the experimental setup is described in detail elsewhere.[16]

RESULTS AND DISCUSSION

In Figure 2, the DINeC mass spectrum from an angiotensin II sample prepared by means of DINeC-Depo (Figure 2b) is

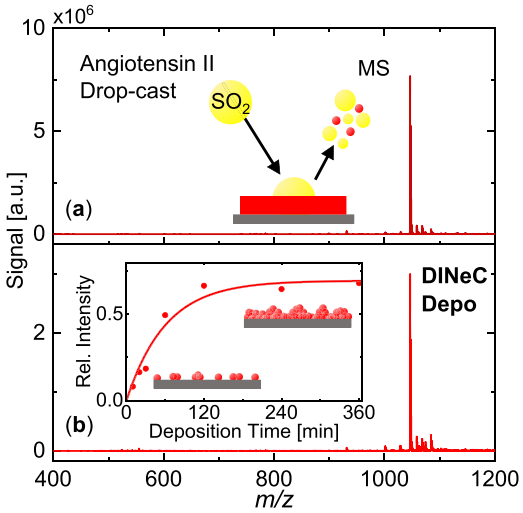

Figure 2. DINeC mass spectra in positive ion mode obtained from angiotensin II (a) drop-cast on SiO_2 and (b) deposited by DINeC-Depo (deposition time t_{depo} = 6 h, d_{ST} = 8 mm). The main peak at m/z = 1046 is assigned to the intact peptide. The intensity of this peak increases with increasing deposition time from 10 min to 6 h (inset). Further peaks occurring at m/z > 1046 are discussed in the main text. Peak positions of all major peaks are listed in Table S1 in the Supporting Information.

compared to a mass spectrum taken from a drop-cast film of angiotensin II (Figure 2a). In both cases, the main peak at m/z = 1046 is assigned to the intact angiotensin II molecule, $[M + H]^+$. Further peaks of much lower intensity are observed in the mass spectrum from the deposited sample at m/z = 1058, 1068, 1074, and 1084. Three of these peaks (m/z = 1058, 1068, and 1084) are also found in the drop-cast sample but show an increased intensity in the spectrum from the deposited sample. The peaks at m/z = 1068 and m/z = 1084 can be assigned to the adduct formation of angiotensin II with alkali metals ($[M + Na]^+$ and $[M + K]^+$, respectively). The peaks at m/z = 1058 and m/z = 1074 are associated with more complex reactions such as esterification or formylation.[28,29] For the former one, the MS/MS spectrum indicates a reaction involving the terminal aspartic acid group of the molecule (Figure S2). Peaks at m/z < 1046 are observed in even lower intensity (<3% of the main peak for both the drop-cast and the

https://doi.org/10.1021/acsomega.3c05518
ACS Omega 2023, 8, 40639−40646

DINeC-Depo sample, compare also the spectra with extended mass range in Figure S3). They can be associated with specific fragments of angiotensin II along the peptide backbone.[23] When we compare the relative intensity of these peaks (with respect to the main peak, which is associated with the intact molecule) in the spectra of the DINeC-Depo samples and in the drop-cast samples, the increase in relative intensity is ≤2%. This increase represents the upper limit for fragmentation induced by the deposition process; it might also originate, at least in part, from other processes, such as reactions on the surface. The deposition by means of DINeC-Depo can thus be seen to be close to fragmentation-free.

The signal intensity of the main peak at m/z = 1046 in the spectra from the deposited samples increases with increasing deposition time (10 min to 6 h, Figure 2b, inset). From the saturation behavior, we conclude a closed layer of angiotensin II molecules to be formed on the substrate after a deposition time of ≈1.5 h in the given configuration. Qualitatively similar mass spectra were measured from angiotensin II deposited on different substrates, e.g., on gold or HOPG substrates (Figures S4a,b in the Supporting Information, respectively).

The amount of molecules deposited by DINeC-Depo was quantified in a QCM experiment. Figure 3 shows the deposited

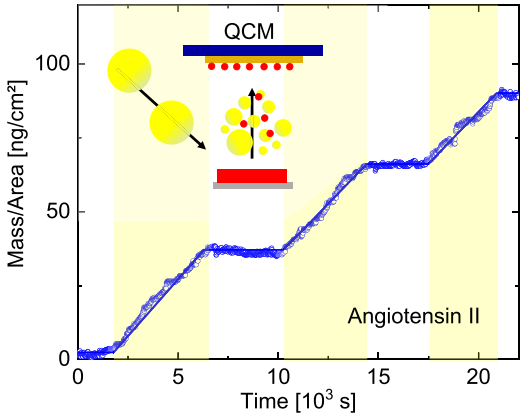

Figure 3. QCM measurement of the mass deposited during a DINeC-Depo experiment with angiotensin II. The QCM plate was installed at a distance of d_{ST} = 30 mm from the target. Yellow-labeled regions indicate that the SO_2 cluster beam was on. Blue open symbols: raw data. Blue straight lines: linear fits within the respective intervals.

mass as recorded on a QCM as a function of the deposition time. The angiotensin II molecules were deposited on the gold electrode (1.3 cm^2) of the quartz crystal resonator, which was installed at the position of the sample at a distance of d_{ST} = 30 mm from the target. When the cluster beam was switched on (t = 1800 s), a continuous increase in the mass was observed. When the beam was turned off again (t = 6300 s), the deposited mass per area was m/A ≈ 37 ng/cm^2 and the respective deposition rate was 7.6 pg/(s·cm^2). In the following period with the beam off (until t = 10,300 s), the recorded mass remained constant. In the second and third deposition cycles, similar deposition rates of 7.1 and 7.0 pg/(s·cm^2) were recorded, respectively; the average deposition rate in this experiment was 7.3 ± 0.3 pg/(s·cm^2) which is considerably lower when compared to the desorption rate of ≈200 pg/(s·cm^2) from a drop-cast angiotensin II sample.[22] We note that the distance between the QCM-plate and the target (d_{ST} = 30 mm) was comparatively large in this experiment; with a lower distance as used in most of the reported experiments, higher deposition rates are achieved. Further improvement of the geometry beyond the current setup (reduced nozzle-target distance, optimized angle of incidence of the beam and angle of collection) is estimated to further increase the deposition rate by up to one order of magnitude. This should then allow for the preparation of real multilayers including more complex film compositions.

The signal intensity in the mass spectra from samples deposited via DINeC-Depo changes as a function of measuring time, as shown in Figure 4. For the main peak at m/z = 1046

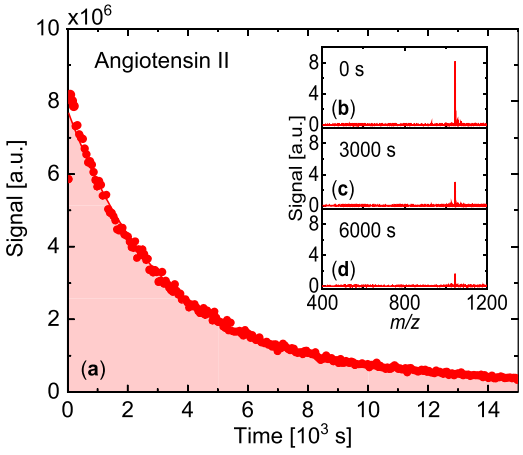

Figure 4. (a) Signal intensity of the peak at m/z = 1046 in DINeC mass spectra from a DINeC-Depo sample (angiotensin II, t_{depo} = 6 h, d_{ST} = 8 mm) as a function of desorption time. The exponential decay results from the removal of the deposited molecules from the SiO_2 surface. (b–d) Positive ion mode DINeC mass spectra were measured at different times as indicated. Peak positions of all major peaks and their intensities are listed in Table S2 in the Supporting Information.

([M + H]$^+$) as measured on a sample of angiotensin II deposited on a silicon wafer for 6 h, the continuous decrease of the signal suggests a film in the (sub-) monolayer regime. On the other hand, from the saturation of the initial signal intensity (Figure 2b, inset), one expects a closed film of several molecular layers in thickness, in accordance with the QCM measurements. We thus conclude that the amount of substance deposited, which corresponds to approximately 3–4 monolayers, is not arranged in well-ordered multilayers but a rather inhomogeneous mode of growth, including islands and clusters of molecules on the surface, is operative. The arrangement of the molecules on the surface might be further influenced by the transfer through ambient conditions, although no major difference was observed when samples that were transferred through the ambient were compared to samples that were transferred between the deposition and analysis chambers without breaking the vacuum.

As some of the molecules that are desorbed via cluster-surface impact carry additional SO_2 molecules as remainders of the cluster fragments in which they were dissolved during the desorption process,[18,19] we analyzed the amount of SO_2 on the surface after DINeC-Depo by means of X-ray photoelectron spectroscopy (XPS). If at all, a sulfur content of less than one sulfur atom per angiotensin molecule was detected on the samples (Figure S5). Indeed, the fraction of biomolecules with SO_2 adducts is typically small;[15,30] from our results, we further

https://doi.org/10.1021/acsomega.3c05518
ACS Omega 2023, 8, 40639–40646

conclude that SO_2 from the background gas does not lead to a substantial SO_2 contamination on the surface, either.

When the target substrates are exchanged during the deposition process, mixed layers can be prepared by DINeC-Depo. In the example shown in Figure 5, a mixture of two peptides, angiotensin II and bradykinin 1−7, was deposited. The DINeC-Depo samples with pure substances were prepared by deposition for 6 h from one single target; the mixed sample was prepared by alternating between the two targets every hour, adding up to a total deposition time of 6 h. In the mass spectrum from the drop-cast angiotensin II sample (Figure 5a), the most intense peak at m/z = 1046 is associated with the intact biomolecule $[M + H]^+$. The same is true for the DINeC-Depo sample with angiotensin II only. An additional peak at m/z = 1062 is observed in the mass spectrum (Figure 5b), which was not observed in the angiotensin II spectra shown previously. It is assigned to an oxidation product of the peptide. The main peak in the mass spectrum shown in Figure 5e from the drop-cast sample of bradykinin 1−7 at m/z = 757 is assigned to the intact peptide molecule $[M + H]^+$. Additional peaks of much lower intensity appear at m/z = 769, 779, 785, and 795. The peaks at m/z = 779 and m/z = 795 are assigned to the adduct formation of bradykinin 1−7 with alkali metals ($[M + Na]^+$ and $[M + K]^+$, respectively), whereas the peaks at m/z = 769 and m/z = 785 are associated with more complex reactions, in analogy to the spectrum from angiotensin II shown in Figure 2. The mass spectrum of the DINeC-Depo sample of bradykinin 1−7 (Figure 5d) again shows the most intense peak at m/z = 757 ($[M + H]^+$) indicating the transfer of the intact molecule. In comparison to Figure 5e, one additional peak is observed at m/z = 773, which can be assigned to an oxidation product of the peptide. The spectrum from the mixed sample shown in Figure 5c is dominated by the peaks at m/z = 1046 and m/z = 757, which are assigned to the two intact biomolecules, $[M1 + H]^+$ and $[M2 + H]^+$. They indicate that both molecules are present at the surface in the same order of magnitude. Although the intensity from the pure DINeC-Depo samples of bradykinin 1−7 and angiotensin II are comparable in Figure 5b,d, an intensity ratio of 1:2 is observed for the mixed sample. This deviation from the ratio expected from the ratio of the deposition times of the single components was also observed for other nominal ratios of molecules in the mixed layers (Figure S6). It might be attributed to a slightly different desorption efficiency from the targets, as observed for other peptides as well;[22] alternatively, it could indicate that in the mixed layers of molecules, the desorption/ionization efficiency of the two molecules is different. This might be attributed, e.g., to a different ionization efficiency of one of the molecules in the presence of the second (so-called "matrix effect"[31−34]).

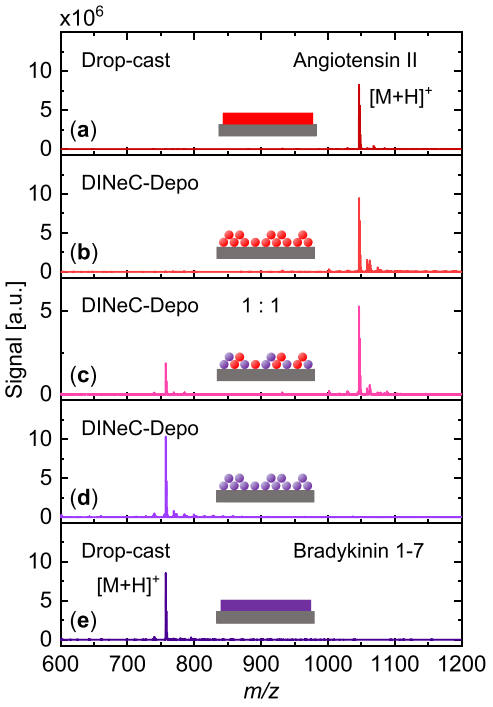

Figure 5. DINeC mass spectra in positive ion mode taken from (a) an angiotensin II sample prepared by drop-casting, (b) an angiotensin II sample prepared by DINeC-Depo, (c) a mixed sample of angiotensin II and bradykinin 1−7 prepared by DINeC-Depo, (d) a bradykinin 1−7 sample prepared by DINeC-Depo, and (e) a bradykinin 1−7 sample prepared by drop-casting. DINeC-Depo samples were prepared by 6 h of deposition (d_{ST} = 12 mm); in the case of the mixed samples, the targets were alternated every hour. The main peaks at m/z = 1046 (a,b) and m/z = 757 (d,e) are assigned to the intact angiotensin II and bradykinin 1−7 molecules, respectively. The mass spectrum from the mixed sample in (c) shows both peaks. Peak positions of all major peaks and their intensities are listed in Table S3 in the Supporting Information.

Similar to angiotensin II, in the spectra taken from the bradykinin 1−7 samples, we find minor peaks at m/z < 757, i.e., the peak associated with the intact bradykinin molecule. They are assigned to specific fragments of the peptide (compare also the spectra with an extended mass range in Figure S7). In analogy to the angiotensin II spectra, we analyzed the increase in the intensity of these peaks, which is below 1% with respect to the main peak, i.e., even lower than in the case of angiotensin II, thus further indicating the soft nature of the desorption/deposition process. At this point, we would like to note that angiotensin II and bradykinin 1−9 have been also investigated by means of deposition via GCIBs.[35] Although experiments with Ar clusters of comparable energy density were performed (Ar^+_{5000}, 1 eV/atom), still about 40% of the molecules were found to be fragmented. The difference might be explained by the very different desorption mechanisms being operative (dissolution- versus impact-based[14,19]), the different desorption/deposition geometries, or a combination of both of them.

As the deposited molecules are in direct contact with the substrate, the cleanliness of the surface plays an important role in the DINeC-Depo experiments. Positive ion mode mass spectra from angiotensin II deposited on differently cleaned SiO_2 surfaces are shown in Figure 6b,c. For comparison, the mass spectrum from a drop-cast film of angiotensin II is shown in Figure 6a. In the latter spectrum, the main peak at m/z = 1046 is associated with the intact peptide ($[M + H]^+$), and adduct and oxidation peaks exhibit an intensity of less than 5% of the main peak. When angiotensin II was deposited on a silicon wafer that was cleaned in an ultrasonic bath (acetone and ethanol, 15 min each, Figure 6b), adduct peaks of higher intensity were observed when compared to the spectrum in Figure 6a. The peak with the highest intensity is observed at m/z = 1084. Along with the peak at m/z = 1066, it is assigned to the adduct formation of angiotensin II with potassium ($[M + K]^+$ and $[M - H_2O + K]^+$, respectively). Sodium adducts (m/z = 1068, $[M + Na]^+$) were also observed

https://doi.org/10.1021/acsomega.3c05518
ACS Omega 2023, 8, 40639−40646

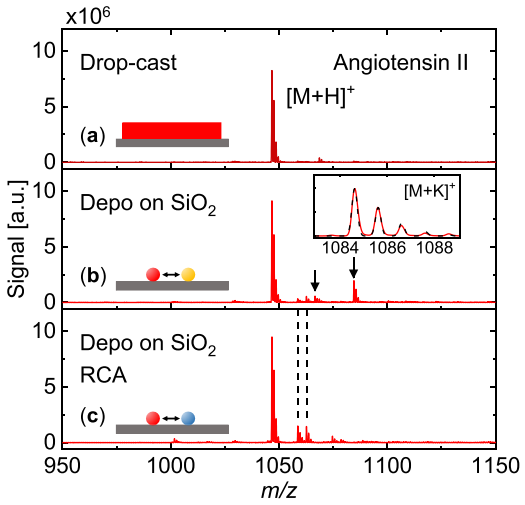

Figure 6. DINeC mass spectra in positive ion mode obtained from angiotensin II samples deposited via DINeC-Depo [(b,c), t_{depo} = 6 h, d_{ST} = 12 mm] on differently cleaned silicon substrates. The mass spectrum from a drop-cast angiotensin II sample is shown in (a) for comparison. In (b), the mass spectrum from a sample prepared by DINeC-Depo on a substrate, which was cleaned in ethanol/acetone only, is shown. Angiotensin II with adducts of potassium ions at m/z = 1084 ($[M + K]^+$) (inset) and m/z = 1066 ($[M - H_2O + K]^+$) is indicated by arrows. In (c), the mass spectrum from a sample deposited on SiO_2 which was additionally cleaned according to the RCA-2-procedure[27] is shown. The adduct peaks are suppressed, and two peaks at m/z = 1058 and m/z = 1062 occur at higher intensities than in the mass spectrum in (b). Peak positions of all major peaks and their intensities are listed in Table S4 in the Supporting Information.

in some experiments. The metal contaminations were almost completely removed from the substrate with an additional cleaning step according to the RCA-2-procedure (Figure 6c). This results in a lower intensity of adduct peaks (<3%). However, in the spectra of the samples prepared on these substrates, the peaks at m/z = 1058 (compare Figure 2) and m/z = 1062 show an increased intensity. The latter is assigned to an oxidation product of angiotensin II.[36] Both peaks are also observed from the drop-cast sample and the samples prepared by DINeC-Depo on substrates cleaned only in ethanol/acetone; however, in the mass spectrum from the samples deposited on the substrates cleaned according to the RCA-2-procedure, they appear with an increased signal intensity of up to ≈15% of the main peak. Additionally, a peak in the mass range m/z < 1046 is observed at m/z = 1001, representing a fragment of the intact peptide ($[M - COOH + H]^+$). The results demonstrate that the peptides, which are in direct contact with the clean SiO_2 surface, are much more prone to further reactions, including oxidation when compared with the molecules in solution or in a drop-cast film.

The degree of oxidation of peptides on samples prepared using DINeC-Depo depends not only on the nature of the substrate but also on handling of the sample after deposition and on the peptides themselves. The peak associated with oxidation of angiotensin II in the mass spectrum shown in Figure 6c (m/z = 1062) is only low in intensity. This changed when the molecule was deposited on a SiO_2 surface which was cleaned according to the RCA-2-procedure[27] and which was installed in the vacuum chamber directly after the cleaning process; a much stronger oxidation of the peptide was observed in this case (compare Figure S4c in the Supporting Information). In comparison, the mass spectrum from bombesin deposited on SiO_2 following the standard cleaning procedure (Figure 7b) shows four prominent peaks separated

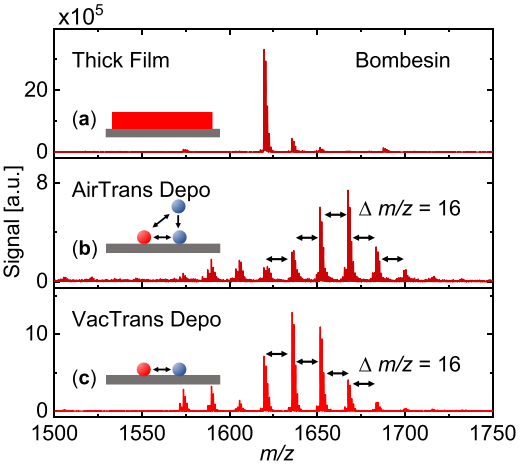

Figure 7. DINeC mass spectra in positive ion mode were obtained from bombesin samples. The mass spectrum from the drop-cast film (a) shows a major peak at m/z = 1619 associated with the intact peptide, $[M + H]^+$. The samples on which the molecules were deposited by DINeC-Depo (t_{depo} = 6 h, d_{ST} = 30 mm) were transferred to the DINeC-MS vacuum chamber via either air (b) or vacuum (c). The mass spectra from these samples show additional peaks separated by $\Delta m/z$ = 16, which are assigned to the oxidation products of the peptide. The peaks at m/z < 1619 are assigned to oxidation products of the bombesin molecule from which the oxidized side group of methionine has been cleaved off (CH_3SOH, $\Delta m/z$ = 64[37,38]). Peak positions of all major peaks and their intensities are listed in Table S5 in the Supporting Information.

by $\Delta m/z$ = 16 each starting from the intact peptide at m/z = 1619 ($[M + H]^+$). The peaks are assigned to oxidation reactions of two of the amino acids, tryptophan and methionine, which are known to be easily oxidized.[39−42] When the sample is transferred between the DINeC-Depo chamber and the DINeC-MS chamber without breaking the vacuum using a mobile vacuum transfer chamber,[43] the peak associated with the intact molecule is observed with higher intensity (Figure 7c) when compared to the spectrum from the sample which was transferred through air. Apparently, atmospheric oxygen enhances the oxidation process. Nonetheless, we also observe a substantial amount of bombesin molecules to be oxidized in the case of the sample which was transferred through vacuum. In that case, the oxidation can be most likely attributed to the influence of SO_2 from the clusters, which, together with H_2O on the sample from the residual gas in the chamber, forms H_2SO_3[18,44] which can readily oxidize the surface-adsorbed molecules during the analysis step as well. Although one might think the same process to be operative during desorption for deposition, the spectra taken from a drop-cast sample (Figure 7a) indicate that on bulk samples the process is much less important. In order to further reduce the influence of the clusters but keep the advantage of the soft desorption process by polar clusters, the use of H_2O clusters might be envisioned; however, this comes at the cost of a more complex cluster source.

So far, we have observed adduct formation and reaction with ambient gases on the surface. In the following, a more complex

https://doi.org/10.1021/acsomega.3c05518
ACS Omega 2023, 8, 40639−40646

reaction between the surface and the molecules that were deposited via DINeC-Depo is illustrated using porphyrins. Bulk samples for this experiment were prepared by drop-casting a saturated ethanolic solution (V = 5−10 μL) on SiO_2 substrates. In the mass spectrum from the drop-cast tetraphenylporphyrin (TPP) sample (Figure 8a), the main peak at m/z = 615 is assigned to the porphyrin molecule ionized by proton uptake, $[M + H]^+$. When the molecule is deposited on silicon oxide by means of DINeC-Depo (Figure 8b), additional peaks separated by $\Delta m/z$ = 16 are observed, which are associated with the oxidation products of the porphyrin. The mass spectrum shown in Figure 8e, which was obtained from a drop-cast sample of copper(II)-tetraphenylporphyrin (CuTPP), features a major peak at m/z = 675, which is assigned to the intact porphyrin $[M]^+$.[45,46] Figure 8d shows the mass spectrum from a sample of CuTPP deposited by means of DINeC-Depo onto a silicon substrate. The peak of the intact molecule is only low in intensity, but a progression of peak groups separated by $\Delta m/z$ = 16 from the most intense peak at m/z = 692 is clearly observed. Similar to the deposition experiment with TPP, these peaks are associated with an oxidation reaction. However, in contrast to oxidation of TPP, the peak progression starts at $\Delta m/z$ = 17 from the peak assigned to the intact CuTPP. This might be interpreted in terms of an additional uptake of a proton when the oxygen atom is incorporated between the copper central ion and one of the nitrogen atoms;[47−50] the oxidation thus goes along with a nominal shift of the ionization process from electron abstraction to proton uptake. Besides the copper-containing species, the peak at m/z = 615 (TPP, $[M + H]^+$) indicates that for some of the molecules copper as the central ion is removed and has been replaced by two protons.

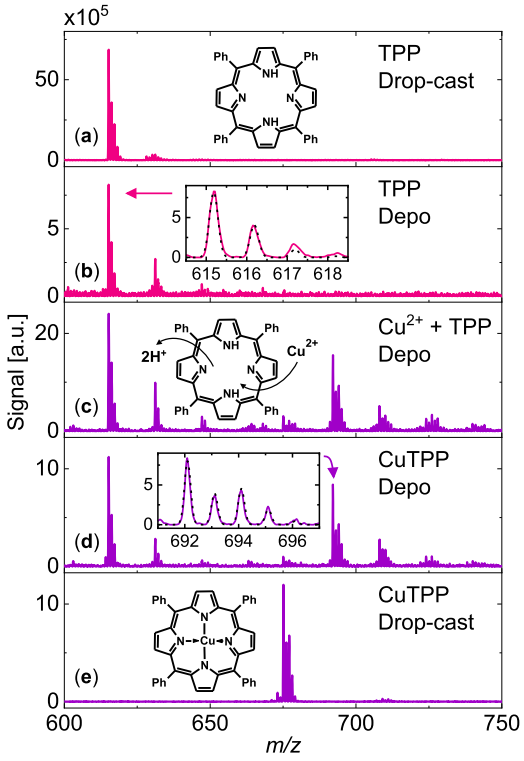

Figure 8. Positive ion mode DINeC mass spectra obtained from two different porphyrins prepared by drop-casting (a,e) or DINeC deposition [(b−d), t_{depo} = 6 h, d_{ST} = 30 mm] on SiO_2. In the mass spectrum from the drop-cast samples, two main peaks are observed at m/z = 615 (a) and m/z = 675 (e), which are assigned to TPP ($[M + H]^+$) and CuTPP ($[M]^+$), respectively.[45] The mass spectra (b−d) from samples prepared by DINeC-Depo also show peaks associated with the intact porphyrins, but additional peak progressions with $\Delta m/z$ = 16, indicating oxidation products, are observed. The mass spectrum in (c) from a sample that was prepared by DINeC-Depo of TPP on $CuCl_2$ shows peaks that are assigned to TPP and CuTPP. Peak positions of all major peaks and their intensities are listed in Table S6 in the Supporting Information.

Finally, TPP was deposited on a $CuCl_2$ surface, which was prepared by drop-casting the salt solution onto the silicon wafer before TPP was deposited via DINeC-Depo on this substrate. The corresponding mass spectrum is shown in Figure 8c; major peaks are observed at m/z = 615 and m/z = 692 accompanied by the corresponding peak progressions. The peak progression at $m/z \geq 675$ indicates the reaction of the porphyrin molecules with the substrate with Cu(II) being integrated into the porphyrin as the central ion; the integrated peak intensity of the peaks associated with CuTPP accounts for approximately 50% of the total peak intensity. Assuming comparable desorption/ionization efficiencies for all of the species investigated, this indicates that about 50% of the deposited TPP molecules were reacted in this way.

CONCLUSIONS

In conclusion, desorption/ionization induced by neutral clusters was introduced as a soft deposition method, which was employed to deposit fragile organic molecules on a variety of different substrates. The process was shown to be fragmentation-free. The amount of material that was deposited ranges from isolated molecules in the submonolayer regime to a few monolayers. As most of the molecules are in direct contact with the substrates and/or the gas phase to which the samples are exposed, reactions with the substrate and/or adsorbates were shown to play a dominant role. Samples prepared by means of DINeC-Depo can thus be used for the investigation of reactions of complex (bio)molecules on surfaces including, among others, adsorbate−adsorbate and adsorbate−surface reactions.

ASSOCIATED CONTENT

Supporting Information

The Supporting Information is available free of charge at https://pubs.acs.org/doi/10.1021/acsomega.3c05518.

Schematic drawing of the DINeC deposition chamber; MS/MS-spectra from the peaks at m/z = 1046 and m/z = 1058 from DINeC-Depo samples of angiotensin II; mass spectra from DINeC-Depo samples of angiotensin II and bradykinin 1−7 with an extended mass range; mass spectra from DINeC-Depo samples of angiotensin II deposited on Au, HOPG, and on activated SiO_2; XPS spectra taken from a DINeC-Depo sample of angiotensin II; intensity ratio of angiotensin II and bradykinin 1−7 peaks in samples mixed via DINeC-Depo as a function of the fraction of the deposition time; and tables of peak positions of all major peaks and their intensities in the shown spectra (PDF)

AUTHOR INFORMATION

Corresponding Author

Michael Dürr − *Institut für Angewandte Physik and Zentrum für Materialforschung, Justus-Liebig-Universität Giessen,*

https://doi.org/10.1021/acsomega.3c05518
ACS Omega 2023, 8, 40639−40646

35392 Giessen, Germany; orcid.org/0000-0002-4676-8715; Email: michael.duerr@ap.physik.uni-giessen.de

Authors

Karolin Pluschke − *Institut für Angewandte Physik and Zentrum für Materialforschung, Justus-Liebig-Universität Giessen, 35392 Giessen, Germany*

Aaron Herrmann − *Institut für Angewandte Physik and Zentrum für Materialforschung, Justus-Liebig-Universität Giessen, 35392 Giessen, Germany*

Complete contact information is available at: https://pubs.acs.org/10.1021/acsomega.3c05518

Notes

The authors declare no competing financial interest.

■ ACKNOWLEDGMENTS

The authors acknowledge financial support from the State of Hesse through the LOEWE Focus Group PriOSS. We thank Jan-Luca Dornseifer and Dr. Joachim Sann for their support in carrying out the XPS measurements.

■ REFERENCES

(1) Catania, F.; de Souza Oliveira, H.; Lugoda, P.; Cantarella, G.; Münzenrieder, N. Thin-film electronics on active substrates: review of material, technologies and application. *J. Phys. D: Appl. Phys.* **2022**, *55*, 323002.

(2) Abegunde, O. O.; Akinlabi, E. T.; Oladijo, O. P.; Akinlabi, S.; Ude, A. U. Overview of thin film deposition technique. *AIMS Mater. Sci.* **2019**, *6*, 174−199.

(3) Zschieschang, U.; Klauk, H. Organic transistors on paper: a brief review. *J. Mater. Chem. C* **2019**, *7*, 5522−5533.

(4) Zou, S.-J.; Shen, Y.; Xie, F.-M.; Chen, J.-D.; Li, Y.-Q.; Tang, J.-X. Recent advances in organic light-emitting diodes: toward smart lighting and displays. *Mater. Chem. Front.* **2020**, *4*, 788−820.

(5) Li, Y.; Huang, W.; Zhao, D.; Wang, L.; Jiao, Z.; Huang, Q.; Wang, P.; Sun, M.; Yuan, G. Recent Progress in Organic Solar Cells: A Review on Materials from Acceptor to Donor. *Molecules* **2022**, *27*, 1800.

(6) Herndon, L. R.; Reid, E. The decomposition of organic compounds at high temperatures and pressures. *J. Am. Chem. Soc.* **1928**, *50*, 3066−3073.

(7) Bank-Srour, B.; Becker, P.; Krasovitsky, L.; Gladkikh, A.; Rosenberg, Y.; Barkay, Z.; Rosenman, G. Physical vapor deposition of peptide nanostructures. *Polym. J.* **2013**, *45*, 494−503.

(8) Rauschenbach, S.; Stadler, F. L.; Lunedei, E.; Malinowski, N.; Koltsov, S.; Costantini, G.; Kern, K. Electrospray Ion Beam Deposition of Clusters and Biomolecules. *Small* **2006**, *2*, 540−547.

(9) Johnson, G. E.; Hu, Q.; Laskin, J. Soft Landing of Complex Molecules on Surfaces. *Annu. Rev. of Anal. Chem.* **2011**, *4*, 83−104.

(10) Portz, A.; Baur, M.; Rinke, G.; Abb, S.; Rauschenbach, S.; Kern, K.; Dürr, M. Chemical analysis of complex surface-adsorbed molecules and their reactios by means of cluster-induced desorption/ionization mass spectrometry. *Anal. Chem.* **2018**, *90*, 3328−3334.

(11) Piqué, A. The matrix-assisted pulsed laser evaporation (MAPLE) process: origins and future directions. *Appl. Phys. A: Mater. Sci. Process.* **2011**, *105*, 517−528.

(12) Lorenz, M.; Shard, A. G.; Counsell, J. D. P.; Hutton, S.; Gilmore, I. S. Angular Distribution of Molecules Sputtered by Gas Cluster Ion Beams and Implications for Secondary Neutral Mass Spectrometry. *J. Phys. Chem. C* **2016**, *120*, 25317−25327.

(13) Delmez, V.; Degand, H.; Poleunis, C.; Moshkunov, K.; Chundak, M.; Dupont-Gillain, C.; Delcorte, A. Deposition of intact and active proteins in vacuo using large argon cluster ion beams. *J. Phys. Chem. Lett.* **2021**, *12*, 952−957.

(14) Delcorte, A. A Microscopic View of Macromolecule Transfer in the Vacuum Using Gas and Bismuth Clusters. *J. Phys. Chem. C* **2022**, *126*, 7307−7318.

(15) Gebhardt, C.; Tomsic, A.; Schröder, H.; Dürr, M.; Kompa, K. Matrix-free formation of gas-phase biomolecular ions by soft cluster-induced desorption. *Angew. Chem., Int. Ed.* **2009**, *48*, 4162−4165.

(16) Baur, M.; Gebhardt, C. R.; Dürr, M. Desorption/ionization induced by neutral cluster impact as a soft and efficient ionization source for ion trap mass spectrometry of biomolecules. *Rapid Commun. Mass Spectrom.* **2014**, *28*, 290−296.

(17) Portz, A.; Bomhardt, K.; Rohnke, M.; Schneider, P.; Asperger, A.; Gebhardt, C. R.; Dürr, M. Soft cluster-induced desorption/ionization mass spectrometry: How soft is soft? *Biointerphases* **2020**, *15*, 021001.

(18) Portz, A.; Baur, M.; Gebhardt, C. R.; Frank, A. J.; Neuderth, P.; Eickhoff, M.; Dürr, M. Influence of the cluster constituents' reactivity on the desorption/ionization process induced by neutral SO_2 clusters. *J. Chem. Phys.* **2017**, *146*, 134705.

(19) Schneider, P.; Verloh, F.; Portz, A.; Aoyagi, S.; Rohnke, M.; Dürr, M. Cluster-induced desorption investigated by means of molecular dynamics simulations - Microsolvation in clusters of polar and non-polar constituents. *J. Chem. Phys.* **2019**, *150*, 214301.

(20) Schneider, P.; Verloh, F.; Dürr, M. Cluster-Induced Desorption/Ionization of Polystyrene: Desorption Mechanism and Effect of Polymer Chain Length on Desorption Probability. *J. Am. Soc. Mass Spectrom.* **2022**, *33*, 832−839.

(21) Lee, B.-J.; Gebhardt, C. R.; Schröder, H.; Kompa, K.-L.; Dürr, M. Observation of ionic desorption channels in cluster-induced desorption of alkali halides − influence of surface electronic properties and surface configuration. *Chem. Phys. Lett.* **2013**, *556*, 77−81.

(22) Portz, A.; Aoyagi, S.; Dürr, M. Soft depth-profiling of mixed peptide/lipid samples by means of cluster induced desorption/ionization mass spectrometry − High depth resolution and low matrix effect. *Biointerphases* **2018**, *13*, 03B405.

(23) Schneider, P.; Keller, P.; Schubert, I.; Bender, M.; Trautmann, C.; Dürr, M. Bond-specific fragmentation of oligopeptides via electronic stopping of swift heavy ions in molecular films. *Sci. Rep.* **2022**, *12*, 17975−17983.

(24) Bomhardt, K.; Schneider, P.; Rohnke, M.; Gebhardt, C. R.; Dürr, M. Cluster-induced desorption/ionization mass spectrometry of highlighter ink: unambiguous identification of dyes and degradation processes based on fragmentation-free desorption. *Analyst* **2022**, *147*, 333−340.

(25) Bomhardt, K.; Schneider, P.; Glaser, T.; Dürr, M. Surface Properties of Ionic Liquids: A Mass Spectrometric View Based on Soft Cluster-Induced Desorption. *J. Am. Soc. Mass Spectrom.* **2022**, *33*, 974−980.

(26) Eusepi, F.; Tomsic, A.; Gebhardt, C. R. Analysis of Solution-Deposited Alkali Ions by Cluster Surface Collisions. *Anal. Chem.* **2003**, *75*, 5124−5128.

(27) Kern, W.; Puotinen, D. Cleaning solutions based on hydrogen peroxide for use in silicon semiconductor technology. *RCA Rev.* **1970**, *31*, 187.

(28) Hesselberth, J. R. Peptide identification and sequenicng by single-molecule detection of peptides undergoing degradation. US Patent, US 20,150,087,526 A1, 2013.

(29) Lecchi, P.; Olson, M.; Brancia, F. L. The role of esterfication on detection of protonated and deprotonated peptide ions in Matrix Assisted Laser Desorption/Ionization (MALDI) Mass Spectrometry (MS). *J. Am. Soc. Mass Spectrom.* **2005**, *16*, 1269−1274.

(30) Baur, M.; Lee, B.-J.; Gebhardt, C. R.; Dürr, M. Soft cluster-induced desorption and ionization of biomolecules—Influence of surface load and morphology on desorption efficiency. *Appl. Phys. Lett.* **2011**, *99*, 234103.

(31) Deline, V. R.; Katz, W.; Evans, C. A.; Williams, P. Mechanism of the SIMS matrix effect. *Appl. Phys. Lett.* **1978**, *33*, 832−835.

(32) Shard, A. G.; Spencer, S. J.; Smith, S. A.; Havelund, R.; Gilmore, I. S. The matrix effect in organic secondary ion mass spectrometry. *Int. J. Mass Spectrom.* **2015**, *377*, 599−609.

(33) Takahashi, K.; Aoyagi, S.; Kawashima, T. TOF-SIMS matrix effects in mixed organic layers in Ar cluster ion depth profiles. *Surf. Interface Anal.* **2017**, *49*, 721−727.
(34) Nakano, S.; Yamagishi, T.; Aoyagi, S.; Portz, A.; Dürr, M.; Iwai, H.; Kawashima, T. Evaluation of matrix effects on TOF-SIMS data of leu-enkephalin and 1, 2-dioleoyl-sn-glycero-3-phosphocholine mixed samples. *Biointerphases* **2018**, *13*, 03B403.
(35) Delmez, V.; Tomasetti, B.; Daphnis, T.; Poleunis, C.; Lauzin, C.; Dupont-Gillain, C.; Delcorte, A. Gas Cluster Ion Beams as a Versatile Soft-Landing Tool for the Controlled Construction of Thin (Bio)Films. *ACS Appl. Bio Mater.* **2022**, *5*, 3180−3192.
(36) Lloyd, J. A.; Spraggins, J. M.; Johnston, M. V.; Laskin, J. Peptide ozonolysis: Product structures and relative reactivities for oxidation of tyrosine and histidine residues. *J. Am. Soc. Mass Spectrom.* **2006**, *17*, 1289−1298.
(37) Guan, Z.; Yates, N. A.; Bakhtiar, R. Detection and characterization of methionine oxidation in peptides by collision-induced dissociation and electron capture dissociation. *J. Am. Soc. Mass Spectrom.* **2003**, *14*, 605−613.
(38) Reid, G. E.; Roberts, K. D.; Kapp, E. A.; Simpson, R. J. Statistical and Mechanistic Approaches to Understanding the Gas-Phase Fragmentation Behavior of Methionine Sulfoxide Containing Peptides. *J. Proteome Res.* **2004**, *3*, 751−759.
(39) Davies, M. J. The oxidative environment and protein damage. *Biochim. Biophys. Acta Gen. Subj.* **2005**, *1703*, 93−109.
(40) Morand, K.; Talbo, G.; Mann, M. Oxidation of peptides during electrospray ionization. *Rapid Commun. Mass Spectrom.* **1993**, *7*, 738−743.
(41) Jeong, K.-H.; Seo, J.; Yoon, H.-J.; Shin, S. K. Focused Electrospray Deposition for Matrix-Assisted Laser Desorption/Ionization Mass Spectrometry. *Bull. Korean Chem. Soc.* **2010**, *31*, 2293−2298.
(42) Schweikart, F.; Hulthe, G. HPLC-UV-MS analysis: A source for severe oxidation artifacts. *Anal. Chem.* **2019**, *91*, 1748−1751.
(43) Länger, C.; Ernst, P.; Bender, M.; Severin, D.; Trautmann, C.; Schleberger, M.; Dürr, M. Single-ion induced surface modifications on hydrogen-covered Si(001) surfaces - significant difference between slow highly charged and swift heavy ions. *New J. Phys.* **2021**, *23*, 093037.
(44) Lee, B.-J.; Baur, M.; Gebhardt, C. R.; Dürr, M. Quantification of the ionization probability during desorption/ionization of oligopeptides induced by neutral cluster impact. *Rapid Commun. Mass Spectrom.* **2013**, *27*, 1090−1094.
(45) Portz, A.; Gebhardt, C. R.; Dürr, M. Real-time investigation of the H/D exchange kinetics of porphyrins and oligopeptides by means of neutral cluster induced desorption/ionization mass spectrometry. *J. Phys. Chem. B* **2017**, *121*, 11031−11036.
(46) Herritsch, J.; Kachel, S. R.; Fan, Q.; Hutter, M.; Heuplick, L. J.; Münster, F.; Gottfried, J. M. On-surface porphyrin transmetalation with Pb/Cu redox exchange. *Nanoscale* **2021**, *13*, 13241−13248.
(47) Yang, F.-A.; Guo, C.-W.; Chen, Y.-J.; Chen, J.-H.; Wang, S.-S.; Tung, J.-Y.; Hwang, L.-P.; Elango, S. ESR, zero-field splitting, and magnetic exchange of exchange-coupled copper(II)-copper(II) pairs in copper(II) tetraphenylporphyrin N-oxide. *Inorg. Chem.* **2007**, *46*, 578−585.
(48) Prigge, S. T.; Eipper, B. A.; Mains, R. E.; Amzel, L. M. Dioxygen Binds End-On to Mononuclear Copper in a Precatalytic Enzyme Complex. *Science* **2004**, *304*, 864−867.
(49) Lewis, E. A.; Tolman, W. B. Reactivity of Dioxygen-Copper Systems. *Chem. Rev.* **2004**, *104*, 1047−1076.
(50) Liu, Y.; Han, Y.; Zhang, Z.; Zhang, W.; Lai, W.; Wang, Y.; Cao, R. Low overpotential water oxidation at neutral pH catalyzed by a copper(II) porphyrin. *Chem. Sci.* **2019**, *10*, 2613−2622.

https://doi.org/10.1021/acsomega.3c05518
ACS Omega 2023, 8, 40639−40646